Available online at www.sciencedirect.com
SCIENCE DIRECT®
International Journal of Heat and Mass Transfer 48 (2005) 2741–2758
International Journal of HEAT and MASS TRANSFER
www.elsevier.com/locate/ijhmt

Relativistic moving heat source

Y.M. Ali *, L.C. Zhang

School of Aerospace, Mechanical, and Mechatronic Engineering, J07, University of Sydney, NSW 2006, Australia

Received 5 December 2003; received in revised form 5 January 2005
Available online 21 March 2005

Abstract

The relativistic heat conduction (RHCE) model is particularly important in the analysis of processes involving moving heat sources (MHS) at speeds or frequencies comparable with those of heat propagation in the medium. This paper establishes a unified framework for solving heat conduction problems using the RHCE model. It offers "Fundamental Solutions" in one, two, and three spatial dimensions, for the transient response due to an instantaneous point MHS. Moreover, it presents the transient response due to a continuous point MHS, the quasi-steady response due a periodic point MHS, as well as guidelines for solving the RHCE equation under various loading and boundary conditions.

Keywords: Relativity; Hyperbolic; Heat; Fundamental solution

1. Introduction

1.1. The relativistic heat conduction model

It is well established that the Fourier equation of heat conduction,

$$\frac{\partial\theta}{\partial t} = \alpha\nabla^2\theta \tag{1}$$

is not compatible with the principles of relativity [1,2], in that it assumes an infinite speed of heat propagation, which is physically inadmissible. The hyperbolic heat conduction equation (HHCE),

$$\frac{1}{C^2}\frac{\partial^2\theta}{\partial t^2} + \frac{1}{\alpha}\frac{\partial\theta}{\partial t} = \nabla^2\theta \tag{2}$$

has been extensively used, because it was thought to be more compatible with the theory of relativity, in the sense that it acknowledges the finite speed of heat propagation, C. Eq. (1) is a parabolic diffusion equation that is always stable, while Eq. (2) is similar in form to the Maxwell (telegraph) equation of an electromagnetic field. It is a wave equation that allows for a range of phenomena, such as reflection, refraction, diffraction, regeneration, resonance, and shock waves; mostly uncommon for a diffusion process like that depicted by Eq. (1). Therefore, Eq. (2) is more interesting, fundamentally.

However, in the transition from Eq. (1) to Eq. (2), it was necessary to change the definition of the heat flux vector, $\boldsymbol{q}$, from Fourier's linear model

$$\boldsymbol{q} = -k\nabla\theta \tag{3}$$

to the more controversial form

$$\tau_0\frac{\partial\boldsymbol{q}}{\partial t} + \boldsymbol{q} = -k\nabla\theta, \tag{4}$$

which is often attributed to Cattaneo [3] and Vernotte [4]. Eq. (4) was derived based on statistical mechanics

* Corresponding author. Tel.: +612 9351 7158; fax: +612 9351 7060.
E-mail address: yali@aeromech.usyd.edu.au (Y.M. Ali).

0017-9310/$ - see front matter © 2005 Published by Elsevier Ltd.
doi:10.1016/j.ijheatmasstransfer.2005.02.004

Nomenclature

C	speed of second sound (heat)
g	fundamental temperature
h	modified temperature
J_0, J_1	Bessel functions of the first kind
k	thermal conductivity
$\boldsymbol{o}$	time unit vector
$\boldsymbol{q}$	heat flux vector
q_g	heat generation rate
Q	dimensionless heat generation
Q_0	heat intensity
R	3-D spatial radius
$\boldsymbol{U}$, U_x	speed of moving medium
U	dimensionless speed
W	dimensionless source frequency
p, q, r, s	image (transformed) space dimensions
t, x, y, z	space–time dimensions/ source position
T, X, Y, Z	dimensionless space–time/ observer position

Greek symbols

α	thermal diffusivity
β	relativistic speed factor
δ	delta (pulse) function
Γ	step function
θ	temperature
ρ	2-D spatial radius
τ_0	relaxation time
ω	source frequency
τ, ξ, ψ, ζ	source-observer distances

Other symbols

∇	gradient operator
∇^2	Laplacian operator
$\Box$	quad operator
$\Box^2$	d'Alembertian operator

and considerations from the kinetic theory of gases [2,5,6], which are all mathematically cumbersome. Furthermore, Eq. (4) was verified neither theoretically nor experimentally [1]. Moreover, it is well established that Eq. (4) can violate at least one statement of the second law of thermodynamics [7–9], and can lead to a number of paradoxical situations.

The relativistic heat conduction (RHCE) model [10] established the validity of Eq. (2) on the basis of the theory of relativity alone, without worrying about any microscopic considerations or material-specific calculations. In fact, the actual mechanism by which heat is transferred through the medium was found to be irrelevant in proving Eq. (2). Yet, to establish Eq. (2) on relativistic grounds, it was necessary to change the definition, Eq. (4), of the heat flux vector to the form

$$\boldsymbol{q} = -k\Box\theta = \frac{\mathrm{i}k}{C}\frac{\partial\theta}{\partial t}\boldsymbol{o} + \alpha\nabla\theta, \tag{5}$$

while rewriting Eq. (2) in the form

$$\frac{\partial\theta}{\partial t} = \alpha\Box^2\theta = \frac{-\alpha}{C^2}\frac{\partial^2\theta}{\partial t^2} + \alpha\nabla^2\theta. \tag{6}$$

It was shown in [10] that Eq. (6) satisfies the second law of thermodynamics, if the heat flux vector is invariant with respect to a Lorentz transformation, which is the case for Eq. (5), but not so for Eq. (4).

To avoid confusion, Eq. (6), which requires Eq. (5), is called the RHCE, while Eq. (2), which requires Eq. (4), is called the HHCE. Both Eq. (6) and Eq. (2) have exactly the same form, but completely different physical and conceptual backgrounds. In particular, the RHCE, thanks to the definition in Eq. (5), is compatible with the theory of relativity *and* the second law of thermodynamics. On the other hand, the HHCE, due to the anomalous structure of Eq. (4), is compatible with relativity only artificially (form not concept), and can violate at least one statement of the second law. Therefore, for the first time, we seem to have a model for heat conduction that is in agreement with *all* known laws of physics.

1.2. Industrial applications

The RHCE model is particularly important for many manufacturing processes, such as continuous annealing after cold working; pulsed-laser cutting and welding; and high speed machining and grinding. In these cases, a moving and/or periodic heat source is applied to the surface of a work-material, to induce geometric and/or structural changes. Technology advances mean that speeds of motion of these heat sources will continue to increase.

As argued in [10], these processes suffer very sharp spatial and temporal temperature gradients. Moreover, the presence of severe plastic deformation and/or phase changes imposes significant drag on the mechanisms of heat propagation. Consequently, speed of heat propagation under these conditions can be very small indeed. While experimental data is scarce, we estimate that under high-speed machining conditions, speed of heat can be in the 1–1000 m/s range. On the other hand, many of the above manufacturing processes operate at speeds within the same range [11]. Therefore, the RHCE model is essential for the proper analysis of these processes.

The literature contains many HHCE models for the moving heat source problem, e.g. [12], but they are all based on Eq. (4), which is shown in [10] to be invalid. The objective of this paper is to reformulate fundamental and general solutions for a variety of heat conduction problems using a relativistic moving heat source (RMHS) model, based on the relativistic definition of the heat flux vector in Eq. (5). Continuous annealing after wire drawing is a typical example of the RMHS problem in one spatial dimension. Pulsed laser applications are examples of periodic RMHS in 2D or 3D. High-speed orthogonal machining is idealized by a continuous RMHS in 2D, while grinding is simulated by a periodic RMHS in 3D. Some of these idealizations are presented in this work, with the objective of establishing a general framework for the solution of a wider class of problems under various loading and boundary conditions. Results obtained from these idealized models will be applied to specific industrial processes, using typical loading and boundary conditions and material properties; and to be published subsequently.

2. The relativistic moving heat source model

Consider a stationary coordinate system, and a rigid continuous medium moving at a constant velocity, U_x, along the positive x-axis. In the absence of heat sources, the relativistic heat conduction equation for a moving medium is [10]

$$\frac{\partial\theta}{\partial t}+U_x\frac{\partial\theta}{\partial x}=\alpha\Box^2\theta, \tag{7}$$

or, in expanded form

$$\alpha\left(\frac{1}{C^2}\frac{\partial^2\theta}{\partial t^2}-\frac{\partial^2\theta}{\partial x^2}-\frac{\partial^2\theta}{\partial y^2}-\frac{\partial^2\theta}{\partial z^2}\right)+\frac{\partial\theta}{\partial t}+U_x\frac{\partial\theta}{\partial x}=0. \tag{8}$$

In the presence of heat generation, whose rate per unit volume is q_g, it becomes

$$\alpha\left(\frac{1}{C^2}\frac{\partial^2\theta}{\partial t^2}-\frac{\partial^2\theta}{\partial x^2}-\frac{\partial^2\theta}{\partial y^2}-\frac{\partial^2\theta}{\partial z^2}\right)+\frac{\partial\theta}{\partial t}+U_x\frac{\partial\theta}{\partial x}=\frac{1}{k}q_g(t,x,y,z), \tag{9}$$

We seek to obtain general solutions for Eq. (9), subject to various boundary conditions and heat sources. The approach adopted in this paper is similar to that adopted by Carslaw and Jaeger [13], and using many of the techniques in [14,15]. In particular, we need to find fundamental solutions of Eq. (9), due to an instantaneous point source, with homogeneous (i.e. zero) initial and boundary conditions. These fundamental solutions are then used to solve many more problems, by convolution and integration over space and time. This procedure is outlined below:

1. We put Eq. (9) in a dimensionless form, that is independent of specific material properties, by introducing the dimensionless quantities

$$T=\frac{C^2}{2\alpha}t,\quad X=\frac{C}{2\alpha}x,\quad Y=\frac{C}{2\alpha}y,\quad Z=\frac{C}{2\alpha}z,$$
$$Q=\frac{4\alpha q_g}{C^2k},\quad U=\frac{U_x}{C},\quad W=\frac{2\alpha\omega}{C^2}. \tag{10}$$

Thus, Eq. (9) is transformed into the dimensionless form

$$\frac{\partial^2\theta}{\partial T^2}-\frac{\partial^2\theta}{\partial X^2}-\frac{\partial^2\theta}{\partial Y^2}-\frac{\partial^2\theta}{\partial Z^2}+2\frac{\partial\theta}{\partial T}+2U\frac{\partial\theta}{\partial X}=Q(T,X,Y,Z). \tag{11}$$

2. We use the method of images [2] to represent any non-homogeneous boundary conditions. This method simply replaces any boundary by an equivalent set of heat sources or sinks. For example, adiabatic boundaries can be simulated by placing a mirror image of the heat sources on the other side of the boundary, thus ensuring zero heat flux across the boundary. Isothermal boundaries are simulated by placing heat sinks on the other side of the boundary, thus ensuring a constant temperature on the boundary. Convection and radiation boundary conditions can be simulated by heat sources or sinks, whose intensity is a function of temperature. The method of images relieves us from the burden of solving for various boundary conditions and geometries, by representing those boundaries as heat sources and lumping-up them all in the right side of Eq. (11).
3. Actually, as will be shown later, boundary conditions are not very important in the RHCE, because the finite speed of heat propagation imposes its own de facto boundaries. In particular, as long as the heat wave front has not reached the physical boundaries, the later are irrelevant. The thermal field acts *as if* it was contained by an adiabatic boundary moving away from the source with a velocity C. After the wave front reaches the physical boundaries, relativistic effects become insignificant, and the solution of the RHCE equation reverts to that of the classical Fourier equation.
4. The principle of superposition applies. Let temperature at point (X,Y,Z) at time T, due to an instantaneous packet of heat released by a source at point (x,y,z) at time t, be $g(T,X,Y,Z|t,x,y,z)$. Then, temperature at (T,X,Y,Z), due to *all* sources, is obtainable by the convolution integral of all the g-functions due to all sources over space and time. Consequently, general solutions to Eq. (11) can be obtained after finding the fundamental solutions for

$$\frac{\partial^2 g}{\partial T^2}-\frac{\partial^2 g}{\partial X^2}-\frac{\partial^2 g}{\partial Y^2}-\frac{\partial^2 g}{\partial Z^2}+2\frac{\partial g}{\partial T}+2U\frac{\partial g}{\partial X}=\delta[\tau]\delta[\xi]\delta[\psi]\delta[\zeta], \tag{12}$$

where the δ function is

$$\delta[a] = 0 \quad \text{for } a \neq 0; \qquad \int_{-\infty}^{\infty} \delta[a]\mathrm{d}a = 1 \tag{13}$$

and

$$\tau = T - t, \quad \xi = X - x, \quad \psi = Y - y, \quad \zeta = Z - z. \tag{14}$$

Thus, the right-hand side of Eq. (12) represents an instantaneous heat pulse at an infinitesimally small point in space.

5. Eq. (12) can be further simplified by defining a function $h(T, X, Y, Z|t, x, y, z)$, such that

$$g \equiv \mathrm{e}^{UX-T}h. \tag{15}$$

Then, Eq. (12) takes the simpler form

$$\frac{\partial^2 h}{\partial T^2} - \frac{\partial^2 h}{\partial X^2} - \frac{\partial^2 h}{\partial Y^2} - \frac{\partial^2 h}{\partial Z^2} + \beta^2 h = \mathrm{e}^{T-UX}\delta[\tau]\delta[\xi]\delta[\psi]\delta[\zeta], \tag{16}$$

where

$$\beta = \sqrt{U^2 - 1}. \tag{17}$$

If we can solve Eq. (16) for h, then, using Eq. (15), we can obtain the solution of Eq. (12) for g. Then, by integration over space and time, we can obtain general solutions for Eq. (11), or back into Eq. (9), which is the general equation for a relativistic moving heat source under any loading or boundary conditions. The fundamental solutions of Eqs. (16) and (12) will be presented in Section 3, while some of the general solutions for Eq. (11), in a 1-D insulated moving wire, will be covered in Section 4.

3. Fundamental solutions

3.1. Relativistic moving wire

Consider an infinitely long, very thin wire, with perfect insulation, such that the one-dimensional approximation applies. The wire is moving in the positive X-direction with a constant velocity U. At time t, a tiny packet of heat is released at point x. We wish to determine the consequent temperature at any point X and time T. In this case, Eq. (16) becomes

$$\frac{\partial^2 h}{\partial T^2} - \frac{\partial^2 h}{\partial X^2} + \beta^2 h = \mathrm{e}^{T-UX}\delta[\tau]\delta[\zeta]. \tag{18}$$

Performing the Laplace Transform of Eq. (18) from T to s, followed by a Fourier Transform from X to p, we obtain

$$h(s, p \mid t, x) = \frac{\mathrm{e}^{-st+t+\mathrm{i}px-Ux}}{p^2 + s^2 + \beta^2}. \tag{19}$$

Using tables for inverse Laplace and inverse Fourier Transforms [14], we go backward from Eq. (19), from p to X, then from s to T, and obtain

$$h(T, X \mid t, x) = \frac{1}{2}\mathrm{e}^{t-Ux}J_0\left(\beta\sqrt{\tau^2 - |\xi|^2}\right)\Gamma(\tau)\Gamma(\tau - |\xi|), \tag{20}$$

where J_0 is Bessel function of the first kind of order zero, and Γ is the step function

$$\Gamma(a) = \begin{cases} 1 & a \geqslant 0 \\ 0 & a < 0. \end{cases} \tag{21}$$

Then, from Eq. (15) we obtain

$$g(T, X \mid t, x) = \frac{1}{2}\mathrm{e}^{-\tau+U\xi}J_0\left(\beta\sqrt{\tau^2 - |\xi|^2}\right)\Gamma(\tau)\Gamma(\tau - |\xi|). \tag{22}$$

When the point source is located at the origin, $x = t = 0$, Eq. (22) reduces to

$$g(T, X \mid 0, 0) = \frac{1}{2}\mathrm{e}^{-T+UX}J_0\left(\beta\sqrt{T^2 - |X|^2}\right)\Gamma(T)\Gamma(T - |X|). \tag{23}$$

When the wire is not moving, $U = 0$, the transient response from Eq. (23) is shown in Fig. 1. This can be best understood when compared with the equivalent solution using a classical (Fourier) equation of heat conduction [13], Fig. 2. The classical solution is singular at the origin ($x = t = 0$), and decays exponentially with distance, and inversely with time. However, the intriguing phenomenon is that, even at $t = 0$, a solution for temperature exists as far as infinity in space and time. In the RHCE solution, the finite speed of heat imposes a restriction on the solution, and confines it to a finite space. First, the solution is finite, even at the origin. Second, the solution does not extend to infinity. For example, at $T = 4$, the heat wave fronts would have reached $X = \pm 4$. Areas of the wire beyond the wave fronts are completely unaware of the heat source and remain unaffected, showing zero change in temperature. The finite region of matter between the two wave fronts clearly has a finite temperature distribution. As the wave fronts spread away from the source, there is an increasing volume of matter contained and, temperature continuously declines. After very long time, the wave fronts approach infinity, and the RHCE solution approaches the classical solution.

Therefore, it can be concluded that *the effect of the finite speed of heat propagation is equivalent to imposing an adiabatic boundary moving away from the source with a speed C*. This effect is demonstrated by the presence of adiabatic bands in several manufacturing processes. This also explains why, in the transient response, actual physical boundary conditions are not important, since the wave front excludes the effects of those boundaries. This is expected, given that Eq. (6) or (8) is, after all, a wave

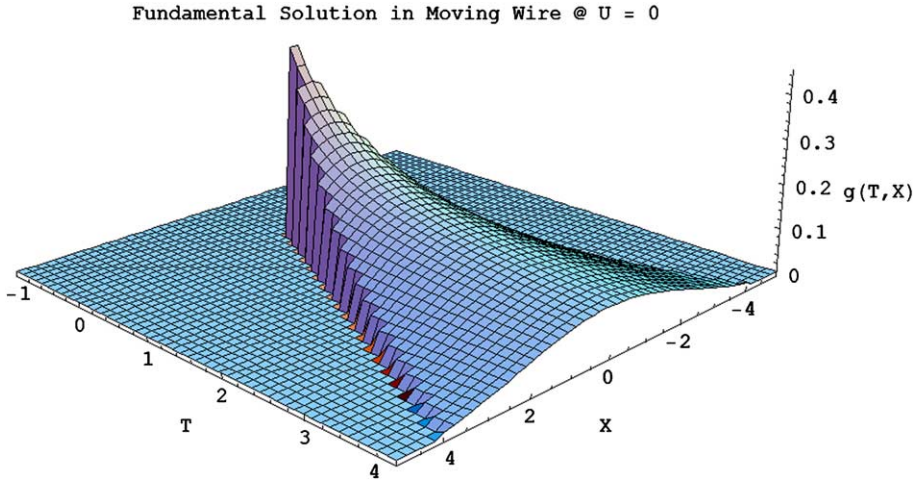

Fig. 1. Fundamental solution due to an instantaneous point source on a moving wire, $U = 0$.

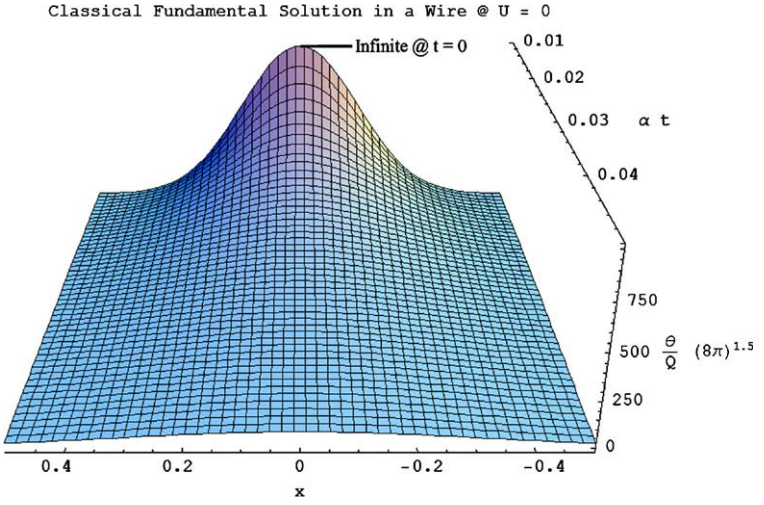

Fig. 2. Classical solution due to an instantaneous point source on a moving wire, $U = 0$.

equation. The presence of the first-order time derivative of temperature, serves only as a dissipative term causing energy content of the wave to diffuse as time passes.

The effect of movement of the medium relative to the source can be understood by inspecting Eq. (11). The effect of speed enters the equation as a first-order derivative with respect to X. Therefore, its effect on the wave propagation is similar to the diffusive effect of the time derivative. However, this effect is anisotropic with respect to the direction of motion. Ahead of the source, it has a dissipative effect, while behind the source it has a generative effect. This can be seen in Fig. 3, where temperature decay downstream is much greater than the decay upstream. At $T = 4$, the heat front is at $X = \pm 4$, while the heat source itself becomes at $X = -2$, effectively convecting heat from one side of the medium to the other side. *The effect of a moving source is equivalent to the convection of heat from downstream to upstream, with a convection coefficient proportional to relative velocity*.

In Fig. 4, the heat source is moving with $U = -1$. At $T = 4$, the wave fronts are at $X = \pm 4$ and the heat source itself is at $X = -4$, just on top of the $-X$ front. Effectively, the $-X$ wave front is annihilated by the source, and all content of the heat source convected towards the $+X$ front. It is also interesting to note that temperature at the $+X$ front becomes constant and does not decay with time. This is because the heat convected upstream is large enough to maintain the $+X$ front at both adiabatic and isothermal conditions.

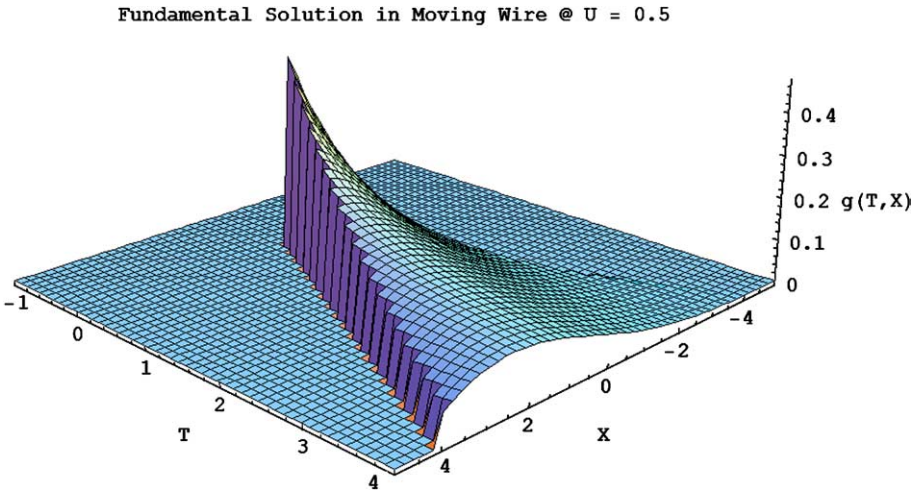

Fig. 3. Fundamental solution due to an instantaneous point source on a moving wire, $U = 0.5$.

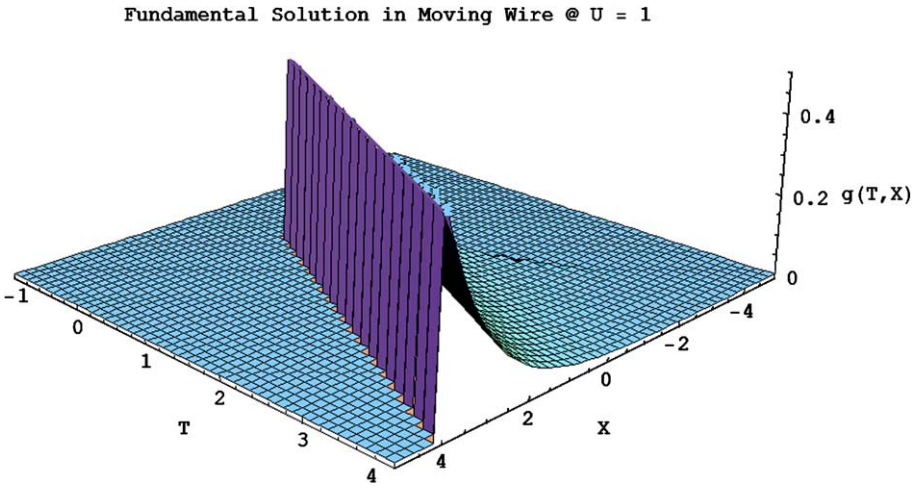

Fig. 4. Fundamental solution due to an instantaneous point source on a moving wire, $U = 1$.

It is important to note here that the heat convection is partially imaginary, and does not actually happen, as can be seen from the relativistic definition of the heat flux vector, Eq. (5). Because of the finite speed of heat propagation, there is a lag in transmission of information about heat. A certain point in the medium is responding to various pieces of information about the heat source, which arrive simultaneously, but are transmitted at different times. This information lag interferes destructively downstream and constructively upstream, thus leading to diminished temperature in one side and a temperature overshoot on the other. This overshoot is clearly demonstrated in Fig. 5, where the heat source is moving at twice the speed of heat propagation. A point of matter below the $+X$ front is receiving false information, about the amount of heat being convected, and accordingly responds by a temperature overshoot. Yet, this overshoot has to be equilibrated by a negative temperature in the wake of the wave front, Fig. 6.

In terms of classical waves, there are speeds of the source at which resonance, shock waves, and negative wakes can occur. The particular feature about heat waves is that they tend to diffuse (correct false information) with the passage of time, and after sufficiently long time, the RHCE model converges to the classical Fourier model.

3.2. Relativistic moving half-plane

Consider a very thin sheet, perfectly insulated on both faces, and extending to infinity in the $X - Z$, $Z \geqslant 0$ half-plane. The thin sheet is moving with a con-

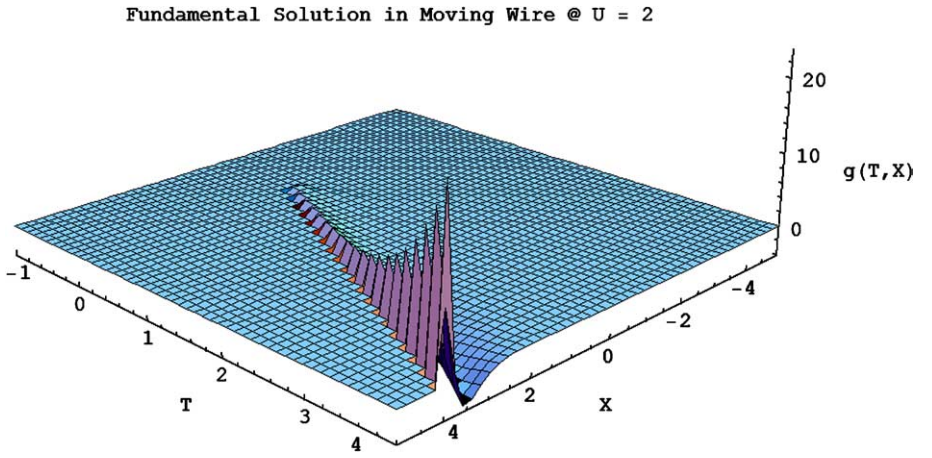

Fig. 5. Fundamental solution due to an instantaneous point source on a moving wire, $U = 2$.

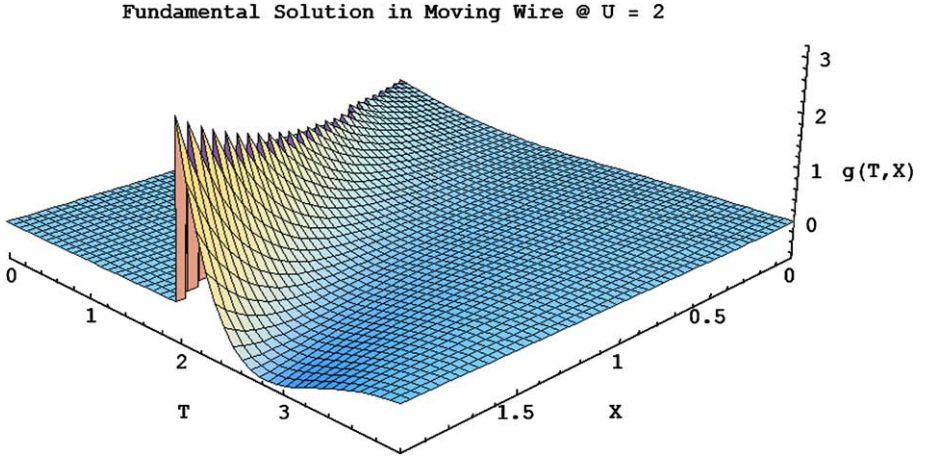

Fig. 6. Cross section on Fig. 5 showing temperature-overshoot and the negative wake.

stant velocity, U, along the $+X$ direction. At time t, a heat packet is released at point (x,z). We wish to find the temperature at any point (X,Z) and time T, in transient response to that heat source. In this case, Eq. (16) becomes

$$\frac{\partial^2 h}{\partial T^2}-\frac{\partial^2 h}{\partial X^2}-\frac{\partial^2 h}{\partial Z^2}+\beta^2 h=\mathrm{e}^{T-UX}\delta[\tau]\delta[\xi]\delta[\zeta]. \tag{24}$$

We take the Laplace transform from T to s, then the Laplace transform from Z to r, then the Fourier transform from X to p, to get

$$h(s,p,r\mid t,x,z)=\frac{\mathrm{e}^{-st+t+ipx-Ux-rz}}{p^2-r^2+s^2+\beta^2}. \tag{25}$$

Using tables for inverse Laplace and inverse Fourier transforms [14], we go backward from Eq. (25), from p to X, then from r to Z and from s to T, to obtain

$$\begin{aligned}&h(T,X,Z\mid t,x,z)\\&=\frac{\mathrm{e}^{t-Ux}\cos\left(\beta\sqrt{-\zeta^2+\tau^2-\mid\xi\mid^2}\right)}{2\pi\sqrt{-\zeta^2+\tau^2-\mid\xi\mid^2}}\\&\quad\times\Gamma(\zeta)\Gamma(\tau)\Gamma(\tau-\mid\xi\mid)\Gamma\left(\sqrt{\tau^2-\mid\xi\mid^2}-\zeta\right).\end{aligned} \tag{26}$$

Then, according to Eq. (15), we get

$$\begin{aligned}&g(T,X,Z\mid t,x,z)\\&=\frac{\mathrm{e}^{-\tau+U\xi}\cos\left(\beta\sqrt{-\zeta^2+\tau^2-\mid\xi\mid^2}\right)}{2\pi\sqrt{-\zeta^2+\tau^2-\mid\xi\mid^2}}\\&\quad\times\Gamma(\zeta)\Gamma(\tau)\Gamma(\tau-\mid\xi\mid)\Gamma\left(\sqrt{\tau^2-\mid\xi\mid^2}-\zeta\right).\end{aligned} \tag{27}$$

If the point source is located at the origin, $t = x = z = 0$, then Eq. (27) simplifies to

$$g(T,X,Z \mid 0,0,0) = \frac{e^{-T+UX}\cos\left(\beta\sqrt{-Z^2+T^2-|X|^2}\right)}{2\pi\sqrt{-Z^2+T^2-|X|^2}} \times \Gamma(Z)\Gamma(T)\Gamma(T-|X|)\Gamma\left(\sqrt{T^2-|X|^2}-Z\right). \quad (28)$$

Due to the three-dimensional nature of Eq. (28), it is difficult to visualize the complete temperature field. We will only consider the temperature field (1) on the surface, $Z = 0$, (2) variation with depth below the origin, $X = 0$, and (3) the spatial distribution at some specific instance in time. Again, the temperature distribution does not extend to infinity in space and time. It is confined within a volume defined by an expanding adiabatic boundary associated with the wave front. In two spatial dimensions, the wave front is actually a semi-circle, with a centre at the origin and a radius running outward with a speed C.

Fig. 7 shows the variation of temperature below the origin, $X = 0$, which naturally decays rapidly with depth below the surface. This variation is independent of the speed of the heat source. Fig. 8 shows temperature distribution in the X–Z plane at a certain time. It shows clearly the wave front spreading radially away from the source. In fact, Eq. (27) can be put in a simpler form, if we define the radius of the wave front

$$\bar{\rho}^2 = \zeta^2 + |\xi|^2, \quad (29)$$

then we have

$$g(T,X,Z \mid t,x,z) = \frac{e^{-\tau+U\xi}\cos\left(\beta\sqrt{\tau^2-\bar{\rho}^2}\right)}{2\pi\sqrt{\tau^2-\bar{\rho}^2}}\Gamma(\zeta)\Gamma(\tau)\Gamma(\tau-\bar{\rho}). \quad (30)$$

Figs. 9–12 show the transient response at the surface, $Z = 0$, at various speeds, which is qualitatively similar to that for a moving wire, Section 3.1. Here again, relative movement of the source creates a bias between upstream and downstream. In the downstream, temperature rise is suppressed, while upstream, it is magnified. At $U = 1$, again, an adiabatic isothermal boundary condition develops along the $+X$ wave front. As speed of the heat source exceeds that of heat propagation, temperature at the wave front overshoots to high values, followed by a negative temperature wave on its wake. Therefore, there seems to be no fundamental difference between the cases of one and two spatial dimensions. It is just that both of the temperature overshoot at the wave front and the negative wake are actually propagating *radially* in the X–Z plane.

3.3. Relativistic moving half-space

Consider the infinite half-space, extending along all of the three spatial dimensions, and confined by the surface $Z \geqslant 0$. An infinitesimal (point) heat source is moving with a constant velocity U along the negative X-axis. At time t, the point source is at point (x, y, z) when it releases a packet of heat. We wish to find the temperature distribution at time T, at any point (X, Y, Z). In this case, the general equation, Eq. (16), applies.

We take the Laplace transform from T to s, then from Z to r. Next, we take the Fourier transform from X to p, then from Y to q, to obtain

$$h(s,p,q,r \mid t,x,y,z) = \frac{e^{-st+t+ipx-Ux+iqy-rz}}{p^2+q^2-r^2+s^2+\beta^2}. \quad (31)$$

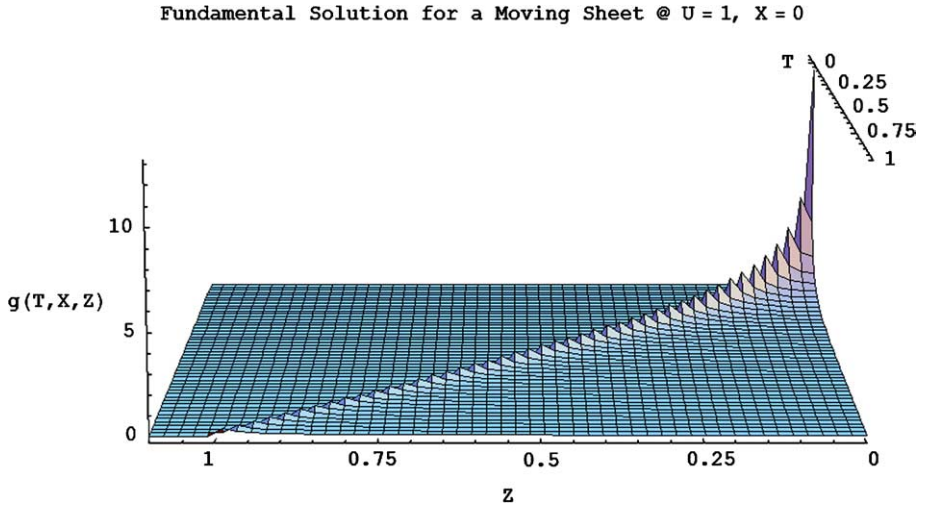

Fig. 7. Fundamental solution in a moving half-plane and depth variation, $U = 1$, $X = 0$.

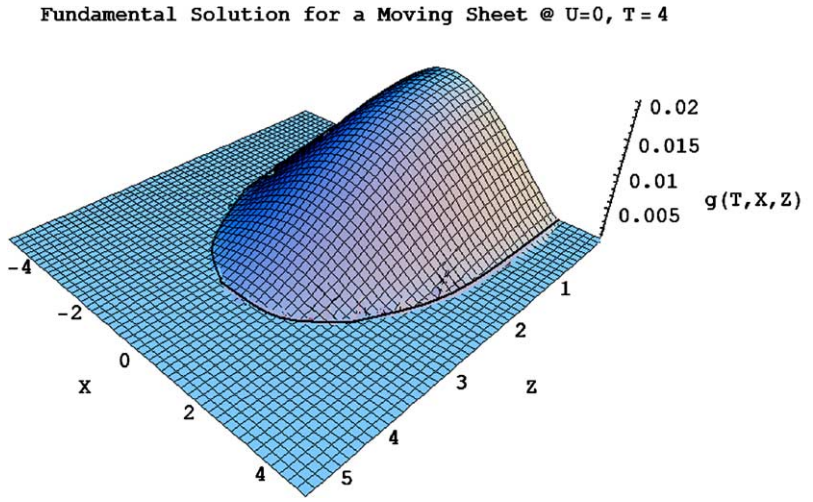

Fig. 8. Fundamental solution in a moving half-plane, spatial distribution, $U = 0$, $T = 4$.

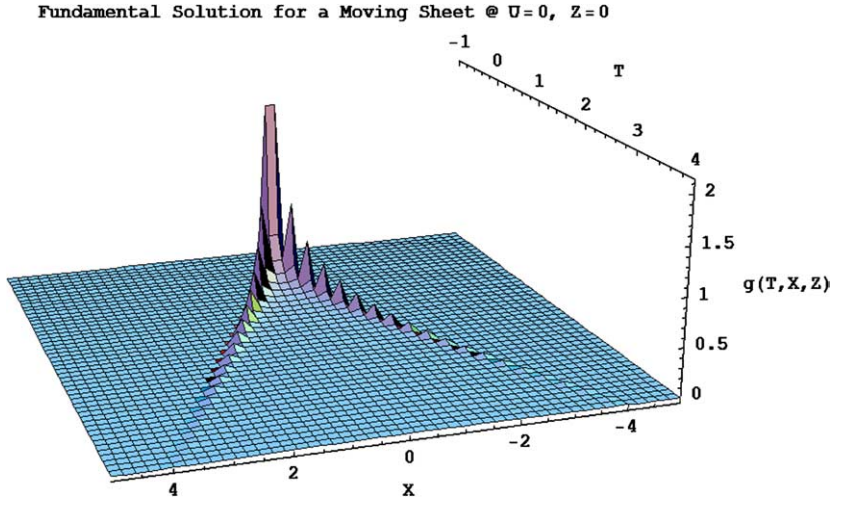

Fig. 9. Fundamental solution on the surface of a moving half-plane, $U = 0$, $Z = 0$.

Using inverse Laplace and Fourier transform tables, we go back from p to X, s to T, r to Z, and q to Y, and finally get

$$h(T,X,Y,Z \mid t,x,y,z) = \frac{e^{t-Ux}}{4\pi}\left(\frac{\delta[\tau-\rho]}{\sqrt{\tau^2-\bar{\rho}^2}} - \frac{\beta\Gamma(\tau-\rho)J_1\left(\beta\sqrt{\tau^2-\rho^2}\right)}{\sqrt{\tau^2-\rho^2}}\right)\Gamma(\tau)\Gamma(\zeta), \tag{32}$$

where J_1 is Bessel function of the first kind of first-order, and

$$\rho^2 = \xi^2+\psi^2+\zeta^2, \quad \bar{\rho}^2 = \xi^2+\zeta^2. \tag{33}$$

Consequently, from Eq. (15), the fundamental solution to Eq. (12) is

$$g(T,X,Y,Z \mid t,x,y,z) = \frac{e^{-\tau+U\xi}}{4\pi}\left(\frac{\delta[\tau-\rho]}{\sqrt{\tau^2-\bar{\rho}^2}} - \frac{\beta\Gamma(\tau-\rho)J_1\left(\beta\sqrt{\tau^2-\rho^2}\right)}{\sqrt{\tau^2-\rho^2}}\right)\Gamma(\tau)\Gamma(\zeta). \tag{34}$$

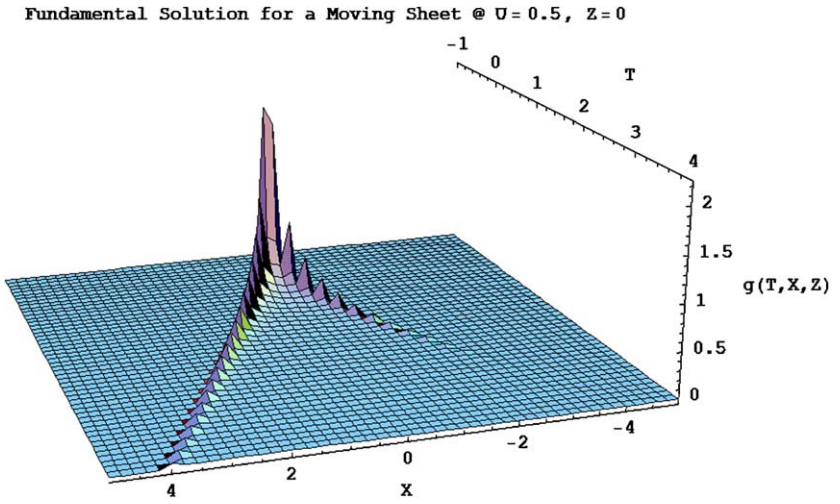

Fig. 10. Fundamental solution on the surface of a moving half-plane, $U = 0.5$, $Z = 0$.

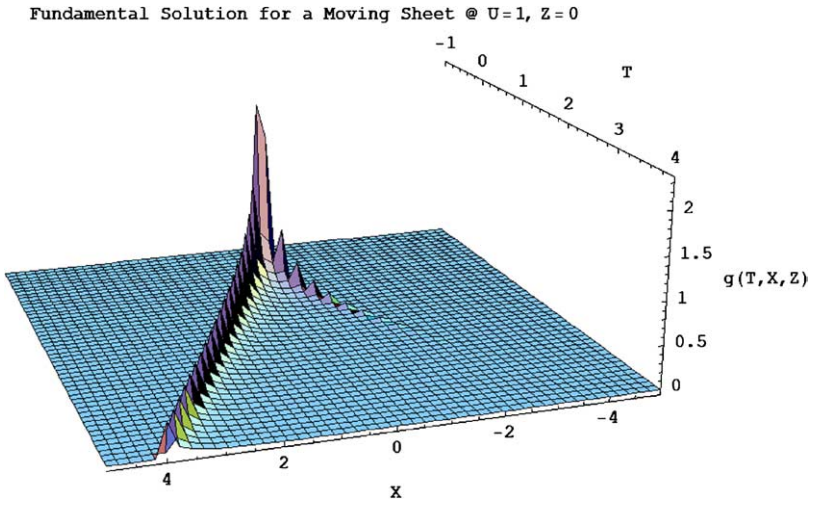

Fig. 11. Fundamental solution on the surface of a moving half-plane, $U = 1$, $Z = 0$.

If the heat source is located at the origin, $t = x = y = z = 0$, then Eq. (34) simplifies to

$$g(T,X,Y,Z \mid 0,0,0,0) = \frac{e^{-T+Ux}}{4\pi}\left(\frac{\delta[T-R]}{\sqrt{T^2-\overline{R}^2}} - \frac{\beta\Gamma(T-R)J_1\left(\beta\sqrt{T^2-R^2}\right)}{\sqrt{T^2-R^2}}\right)\Gamma(T)\Gamma(Z), \quad (35)$$

where

$$R^2 = X^2+Y^2+Z^2, \quad \overline{R}^2 = X^2+Z^2. \quad (36)$$

It is difficult to visualize Eq. (35) graphically, but it poses no fundamental challenge. It is much similar to the behaviour for one and two-dimensional problems. Essentially, the fundamental solution of the RHCE model is the same regardless of dimensionality: *a wave that declines in both frequency and amplitude as it spreads away from the source in space–time*. The effect of dimensionality is only a choice among various trigonometric or Bessel functions used to describe the wave. If we think of some radial axis between the source point and the observation point, then all fundamental behaviour can be observed along that axis. Namely, a wave front spreading away from the source point with a velocity C, the magnitude of the wave de-

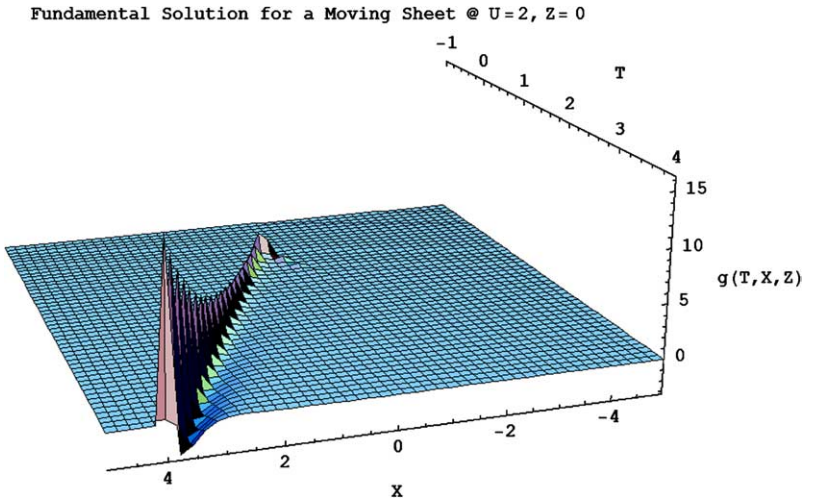

Fig. 12. Fundamental solution on the surface of a moving half-plane, $U = 2$, $Z = 0$.

cays with time and its frequency is also reduced. Movement of the heat source creates a convective effect, causing suppression of temperature on the downstream and temperature overshoot (and possibly a negative wake) on the upstream.

4. General solutions in a moving wire

Now, that we obtained fundamental solutions of the RHCE equation, for various dimensions, it is now possible to obtain general solutions for any type of loading. The fundamental solution is the transient response due to an instantaneous point source. In case of multiple sources, or sources that extend over lines, areas, or volumes, we simply integrate individual fundamental solutions, due to each point source, over space. If the heat source intensity is a function of time, we obtain the general solution by convolving the fundamental solution with the time function for intensity. This process is mathematically straightforward. In many cases, the integration can be obtained in closed-form. In other cases, numerical integration may be more convenient. For very complex geometries, a finite element formulation may be needed.

In this section, we present general solutions for the continuous and for the periodic moving point sources in a wire. This choice is because

(a) It is two dimensional and easy to visualize graphically,
(b) The higher dimension problems do not pose any additional conceptual difficulty,
(c) The RHCE transient response is mostly independent of the details of geometry and boundary conditions, and
(d) It is possible to simulate any time-dependent heat history by the linear superposition of a number of periodic and/or continuous heat sources.

4.1. Continuous moving point source

Consider the problem described in Section 3.1. However, instead of the source being an instantaneous packet released at t, the heat source becomes continuous from t to T and has intensity Q_0. Temperature at any point in the wire is obtained by the convolution of Q_0 with the fundamental solution given in Eq. (22). That is

$$\theta(T,X) = \frac{Q_0}{2}\int_0^T \mathrm{e}^{t-T-Ux+UX} J_0\left(\beta\sqrt{(T-t)^2-\xi^2}\right) \times \Gamma(T-t)\Gamma(T-t-|\,\xi\,|)\,\mathrm{d}t \tag{37}$$

or after some re-arrangement

$$\theta(T,X) = \frac{Q_0\mathrm{e}^{U\xi}}{2}\Gamma(\tau)\Gamma(\tau-|\,\xi\,|) \times \int_\xi^T \mathrm{e}^{-\tau} J_0\left(\beta\sqrt{\tau^2-\xi^2}\right)\mathrm{d}\tau. \tag{38}$$

If the source is located at the origin, $t = x = 0$, Eq. (38) becomes

$$\theta(T,X) = \frac{Q_0\mathrm{e}^{UX}}{2}\Gamma(T)\Gamma(T-|\,X\,|) \times \int_\xi^T \mathrm{e}^{-\tau} J_0\left(\beta\sqrt{\tau^2-\xi^2}\right)\mathrm{d}\tau. \tag{39}$$

Perhaps, it would be useful to consider, first, the classical solution for the continuous point source in a moving wire [1], as shown in Fig. 13. First, the solution extends to infinity in both directions. Second, while temperature decays in the downstream, it remains constant upstream.

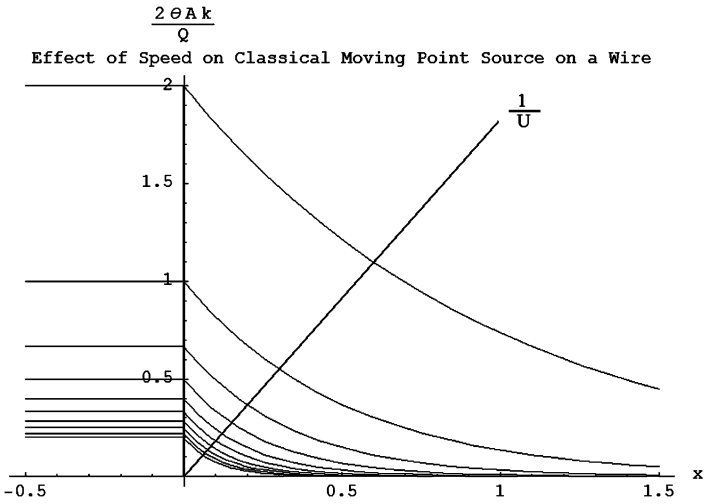

Fig. 13. Quasi-steady temperature distribution due to a "classical" point source moving along $+x$-axis of an insulated wire.

The only effect of the speed of the point source is an inversely proportional scaling down on temperature, simply because at higher speed there is more volume per unit heat. This is to be compared with Figs. 14–18, which show the transient response due to a continuous point RMHS at various velocities.

There are a number of interesting points to be noted

1. The relativistic model predicts a continuously increasing temperature field, e.g. Fig. 14. This is naturally expected, given that the wire is perfectly insulated and there is continuous supply of heat. Because of the finite speed of heat propagation (adiabatic condition at the wave fronts), the wire is no longer of infinite length, and temperature has to rise with time. The rise, however, occurs at a decreasing rate, because the volume contained between the two wave fronts is also increasing with time.
2. Just like the instantaneous response, Section 3.1, the effect of source speed is the convection of heat from downstream to upstream, causing temperature build-up on the upstream and behind the $+X$ wave front. When there is no source motion, $U = 0$, Fig. 14, the temperature field is symmetric. However, as speed increases, Fig. 15 and Fig. 16, the quasi-steady relativistic field resembles the classical field. Indeed, for $U < 1$, we can see that, after very long time, the wave fronts approach infinity and the temperature distribution in Fig. 16 approaches that in Fig. 13.

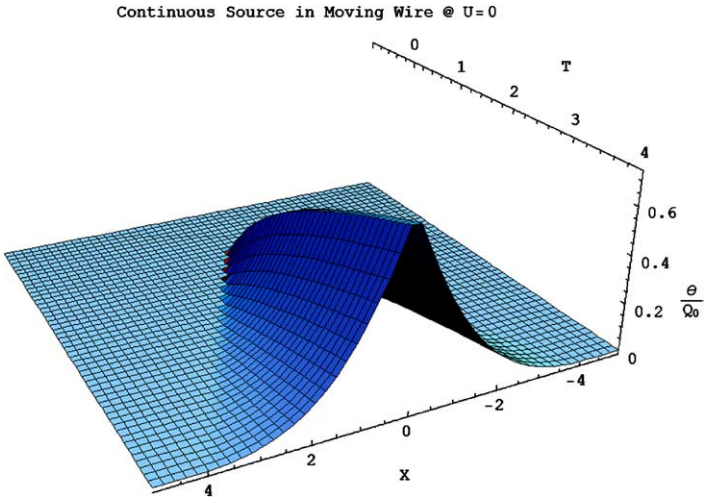

Fig. 14. Continuous point source on a moving wire, $U = 0$.

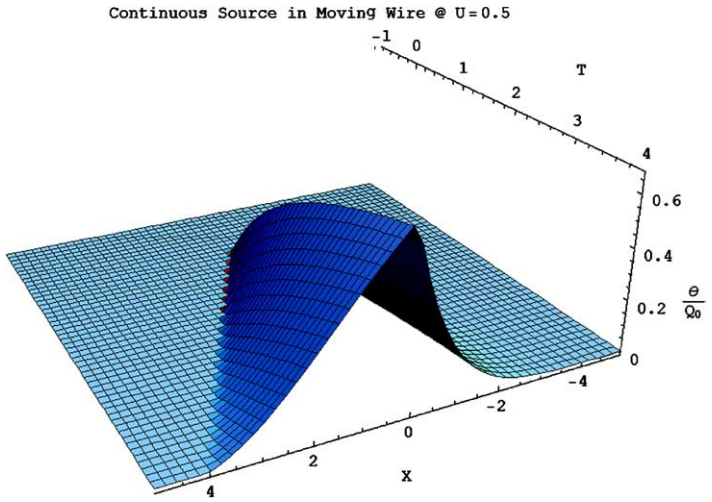

Fig. 15. Continuous point source on a moving wire, $U = 0.5$.

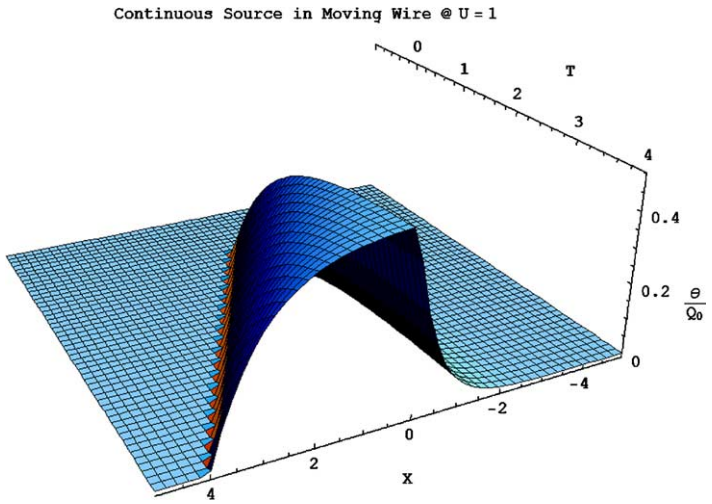

Fig. 16. Continuous point source on a moving wire, $U = 1$.

3. While the classical solution is sensitive to source speed only as a scaling factor, the relativistic solution is more critically sensitive to source speed. For $U > 1$, there is a temperature overshoot at the wave front followed by a negative temperature region in its wake, Figs. 17 and 18. This is exactly the same behaviour as for the instantaneous point source.
4. Temperature overshoot at the wave front and the negative wake have no upper limit and continue to increase as U continues to increase above one. This is clear from comparing the temperature scales in Fig. 17 and Fig. 18. Moreover, temperature continues to rise at the wave front with the progression of time, even for the same source speed.

It is not hard to contemplate the devastating effects that may arise in a manufacturing process, e.g. machining, in which a continuous heat source runs on the surface of a medium with a speed higher than the speed of heat propagation. For example, with one point, at the wave front, expanding rapidly while another point at the wake contracting, there can be severe thermal stresses and damage to the structure of the material. If this thermal overshoot is allowed to continue, soon the material will reach the melting point, or some other major phase change. These phase changes are likely to change thermal properties of the medium, including speed of heat propagation, and prevent this catastrophic behaviour from continuing.

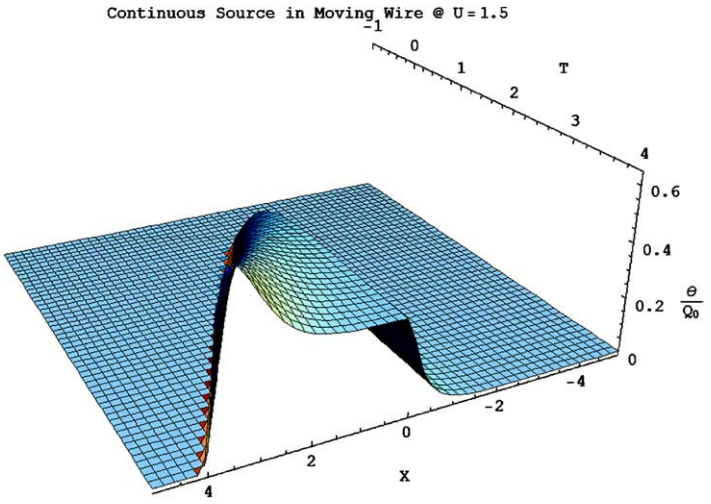

Fig. 17. Continuous point source on a moving wire, $U = 1.5$.

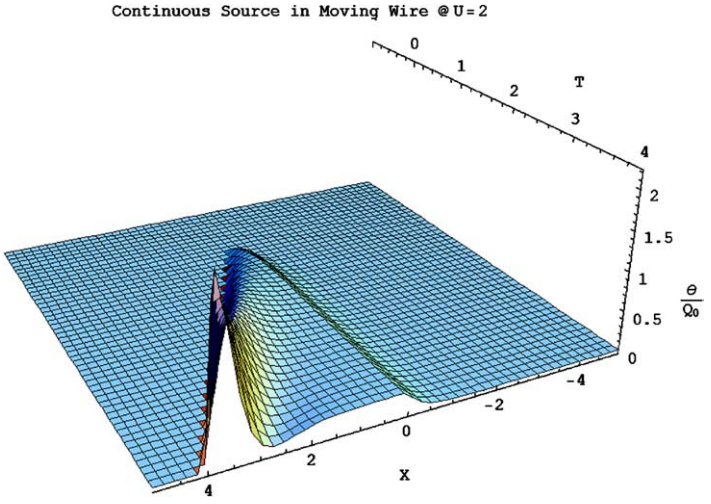

Fig. 18. Continuous point source on a moving wire, $U = 2$.

4.2. Periodic moving point source

Consider the problem described in Section 3.1. However, instead of the source being an instantaneous packet released at t, the heat source becomes a periodic function of the form

$$Q = Q_0 e^{i\mathcal{W}t} = Q_0(\cos[\mathcal{W}t] + i\sin[\mathcal{W}t]). \tag{40}$$

Here, it is interesting to compare Eq. (40) with the relativistic definition of the heat flux vector, Eq. (5). The heat flux is a complex number that has a real component along the spatial gradients and an imaginary component along the temporal gradient. The corresponding components are shown in Eq. (40). This indicates that, in general, temperature is also a complex number, which is expected, since heat is a wave phenomenon whose behaviour can suffer phase-lag and other wave-like behaviour, when subjected to a periodic loading.

As usual, temperature at any point (T, X), due to a periodic point heat source at point x and starting at $T = t$, is obtained by the convolution of the load function, Eq. (40), and the fundamental solution, Eq. (22). That is

$$\theta(T,X) = \frac{Q_0}{2}\int_0^T e^{t-T+i\mathcal{W}t+U\xi} J_0\left(\beta\sqrt{(T-t)^2-\xi^2}\right) \times \Gamma(T-t)\Gamma(T-t-|\,\xi\,|)\,dt \tag{41}$$

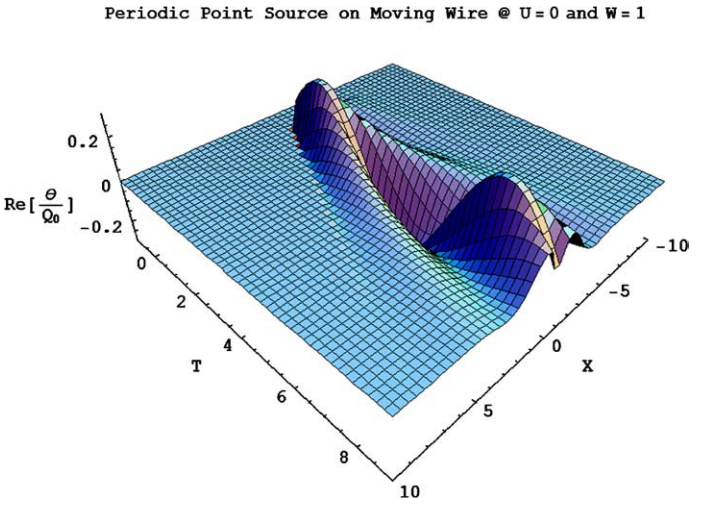

Fig. 19. Quasi-steady periodic response in a stationary wire, $W = 1$.

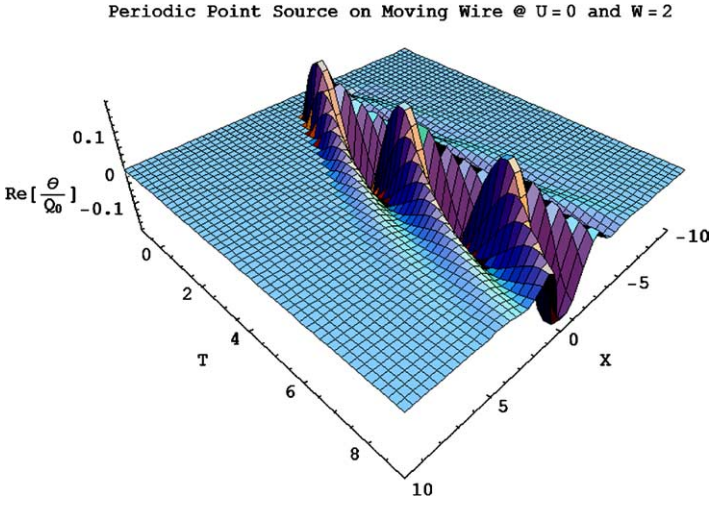

Fig. 20. Quasi-steady periodic response in a stationary wire, $U = 0$, $W = 2$.

or, after some rearrangement

$$\theta(T,X) = \frac{Q_0 e^{iWT+U\xi}}{2}\Gamma(\tau)\Gamma(\tau - |\,\xi\,|) \times \int_{\xi}^{T} e^{-\tau(1+iW)} J_0\left(\beta\sqrt{\tau^2-\xi^2}\right) dt. \quad (42)$$

After sufficiently long time, $T \to \infty$ and $T \gg \xi$, a quasi-steady-state prevails, for which the integral in Eq. (42) approaches a Laplace transform from t to $1 + iW$. Consequently, in the quasi-steady-state, temperature is given by

$$\theta(T,X) = \frac{Q_0 e^{iWT+U\xi-\mathrm{Abs}[\xi]\sqrt{U^2-1+(1+iW)^2}}}{2\sqrt{U^2-1+(1+iW)^2}}, \quad (43)$$

or if the source is located at the origin, $x = 0$,

$$\theta(T,X) = \frac{Q_0 e^{iWT+UX-\mathrm{Abs}[X]\sqrt{U^2-1+(1+iW)^2}}}{2\sqrt{U^2-1+(1+iW)^2}}. \quad (44)$$

As predicted earlier, temperature in Eq. (43) or (44) is indeed a complex number.

From inspection of Eq. (40), we can see that the real component of the temperature field is driven by a cosine wave, while the imaginary component is driven by a sine wave. Both waves are identical except for a $\pi/2$ phase shift. This is, in fact, the case for all plots of the temperature distribution in Eq. (44): the imaginary component

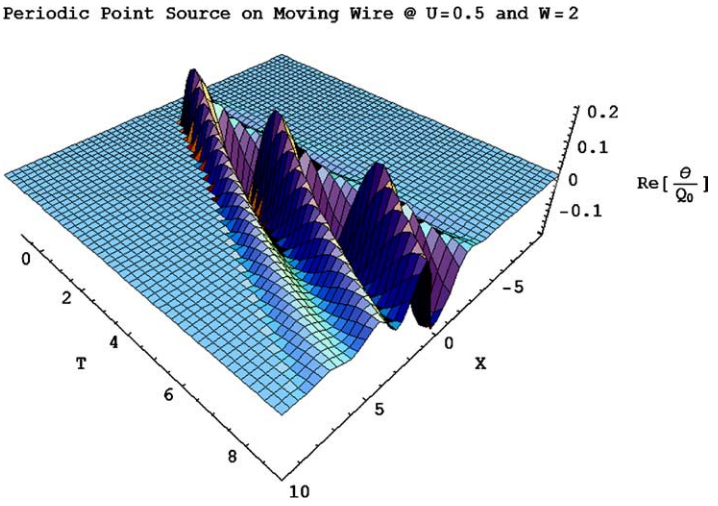

Fig. 21. Quasi-steady periodic response in a moving wire, $U = 0.5$, $W = 2$.

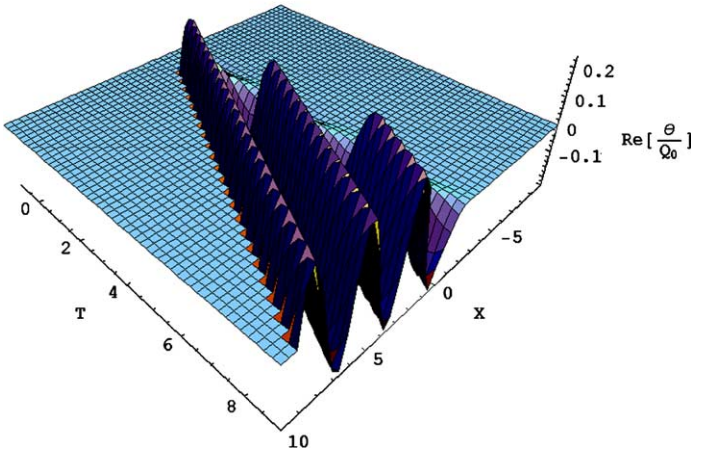

Fig. 22. Quasi-steady periodic response in a moving wire, $U = 1$, $W = 2$.

is identical in shape to the real component except for a $\pi/2$ phase shift. Therefore, due to space limitations, we will show only the real component of the temperature field.

At zero frequency, $W = 0$, the integral in Eq. (42) is identical to the integral in Eq. (38), i.e. a zero-frequency periodic source is just the same as the continuous point source in Section 4.1. Actually, it is easy to shown that Eq. (44), with $W = 0$, is also the quasi-steady-state solution for the continuous point source. Moreover, Eq. (44), with $W = 0$, is similar in form to the quasi-steady *classical* solution for a continuous point source.

At non-zero source frequency, the quasi-steady temperature field is that of a standing wave localized around the source point. It continues to change in time, completely in phase with the source at the source point, and increasingly out of phase at other locations further away from the source, Fig. 19. However, and as expected, due to diffusive nature of the wave, it does not spread far away from the source along the wire.

The effect of increased source frequency is an identical increase in temperature frequency, as can be seen by comparing Fig. 19 and Fig. 20. The effect of source speed is similar to that in all previous cases. As source speed increases, it creates a bias in the field, with more heat going upstream than downstream. This is demonstrated in Fig. 21, where the wave is drifting more in the upstream while being diminished in the downstream. Again, at $U = 1$, the wave does not decay in magnitude, Fig. 22, while at source velocities higher than that critical speed, there can be one or more temperature overshoots and wakes, Fig. 23. The number and phase of those peaks and wakes depend on the source frequency.

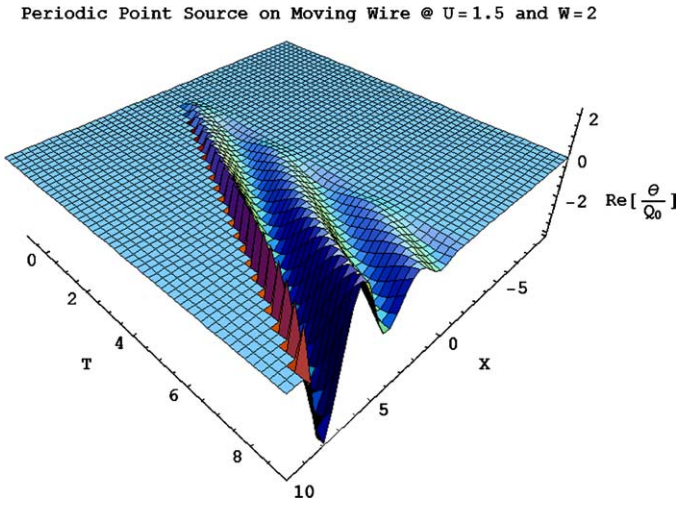

Fig. 23. Quasi-steady periodic response in a moving wire, $U = 2$, $W = 2$.

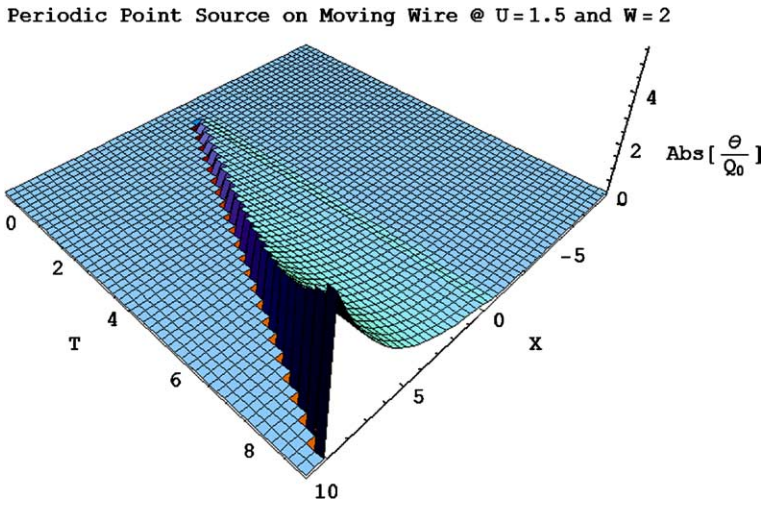

Fig. 24. Absolute (observable) temperature, whose real component is Fig. 23.

Finally, one might ask, what do thermometers and thermocouple measure, the real or the imaginary component of the temperature? Given the similarity between the RHCE model and some aspects of the wave function from quantum mechanics, it would seem that thermocouples measure the "observable", i.e. the amplitude or absolute value of temperature. This can be obtained by multiplying Eq. (44) by its complex conjugate. For, example, Fig. 24 shows the temperature amplitude for the same conditions as those in Fig. 23.

5. Conclusion

Relativistic heat conduction is a description of heat propagation that is much similar to classical wave mechanics, electrodynamics, and quantum mechanics. A heat source emits a wave that propagates radially, with a speed C, away from the source in a 4-D space–time. The wave front acts as an adiabatic boundary condition, preventing the temperature field from running ahead of the heat flux field. Meanwhile, the wave is diffusive, and both of its magnitude and frequency decay as the wave spreads outward. If left alone, or in the quasi-steady-state, the wave front approaches infinity, and the temperature field approaches the one predicted from the classical theory. However, the presence of fast-moving heat sources and/or high frequency excitations, give rise to relativistic effects similar to those observed in wave mechanics. This is mainly due to the possibility of the presence of a phase lag between the temperature and heat flux fields, as manifested by their complex number

presentation. The effect of source movement is to create a bias upstream with the possibility of temperature overshoot. All of these effects can have catastrophic implication in many practical situations.

References

[1] E.R.G. Eckert, R.M. Drake, Analysis of Heat and Mass Transfer, McGraw-Hill Kogakusha, Tokyo, 1972.
[2] P.M. Morse, H. Feshback, Methods of Theoretical Physics, McGraw-Hill, New York, 1953.
[3] C.R. Cattaneo, Sur une de l'équation de la chaleur éliminant le paradoxe d'une propagation instantanée, Compte. Rend. 247 (4) (1958) 431–433.
[4] P. Vernotte, Les paradoxes de la theorie continue de l'équation de la chaleur, Compte. Rend. 246 (22) (1958) 3154–3155.
[5] A.H. Ali, Statistical mechanical derivation of Cattaneo's heat flux law, J. Thermophys. Heat Transfer 13 (4) (1999) 544–546.
[6] M. Chester, Second sound in solids, Phys. Rev. 131 (15) (1963) 2013–2015.
[7] C. Bai, A.S. Lavine, On hyperbolic heat conduction and the second law of thermodynamics, J. Heat Transfer, Trans. ASME 117 (2) (1995) 256–263.
[8] A. Barletta, E. Zanchini, Hyperbolic heat conduction and local equilibrium: a second law analysis, Int. J. Heat Mass Transfer 40 (5) (1997) 1007–1016.
[9] M.B. Rubin, Hyperbolic heat conduction and the second law, Int. J. Eng. Sci. 30 (11) (1992) 1665–1676.
[10] Y.M. Ali, L.C. Zhang, Relativistic heat conduction, Int. J. Heat Mass Transfer, in press, doi:10.1016/j.ijheatmasstransfer.2005.02.003.
[11] L. Zhou, J. Shimizu, A. Muroya, H. Eda, Material removal mechanism beyond plastic wave propagation rate, Precision Eng. 27 (2) (2003) 109–116.
[12] N.S. Al-Huniti, M.A. Al-Nimr, M. Naji, Dynamic response of a rod due to a moving heat source under the hyperbolic heat conduction model, J. Sound Vibrat. 242 (4) (2001) 629–640.
[13] H.S. Carslaw, J.C. Jaeger, Conduction of Heat in Solids, second ed., University Press, Oxford, 1959.
[14] W. Magnus, F. Oberhettinger, Formulas and Theorems for the Functions of Mathematical Physics, Chelsea Publishing, New York, 1949.
[15] D.G. Duffy, Green's Functions with Applications, Chapman and Hall/CRC, Boca Raton, FL, 2001.